

# A METHOD FOR CORRECTION OF ELASTIC AND PIEZOELECTRIC CONSTANTS OF CRYSTALS USING MEASURED SURFACE ACOUSTIC WAVE PARAMETERS

Ernest Brzozowski

Institute of Electronic Materials Technology, 133 Wolczynska Str., 01-919 Warsaw, Poland  
e-mail: ernest.brzozowski@itme.edu.pl

Surface acoustic wave (SAW) properties of a crystal depend on the density, elastic, piezoelectric and dielectric constants. On the basis of literature data, calculations of SAW parameters in a neodymium calcium oxoborate  $[\text{NdCa}_4\text{O}(\text{BO}_3)_3]$  crystal were carried out to evaluate orientations optimal for the correction of elastic and piezoelectric constants. SAW velocities and electromechanical coupling coefficients were measured using SAW delay lines deposited on differently oriented crystal substrates. Dielectric constants were determined from measured effective permittivities. Both a nonlinear least squares algorithm and a computer program for the correction of elastic and piezoelectric constants from measured SAW velocities and electromechanical coupling coefficients were developed. The correction of  $\text{NdCa}_4\text{O}(\text{BO}_3)_3$  elastic and piezoelectric constants was carried out. It was shown that for the corrected constants the differences between the measured and calculated SAW parameters are marginal.

**Key words:** elastic constants, piezoelectric constants, dielectric constants, SAW

## Metoda korekcji stałych elastycznych i piezoelektrycznych kryształów z wykorzystaniem zmierzonych parametrów akustycznych fal powierzchniowych

Własności akustycznych fal powierzchniowych (AFP) w kryształach zależą od gęstości stałych elastycznych, piezoelektrycznych i dielektrycznych. Na podstawie danych z literatury obliczono parametry AFP w kryształach tlenoboranu neodymowo-wapniowego  $[\text{NdCa}_4\text{O}(\text{BO}_3)_3]$  w celu wyznaczenia orientacji optymalnych do korekcji stałych. Zmierzono prędkości i współczynniki sprzężenia elektromechanicznego AFP z wykorzystaniem linii opóźniających osadzonych na podłożach  $\text{NdCa}_4\text{O}(\text{BO}_3)_3$  o różnych orientacjach. Wyznaczono stałe dielektryczne z pomiaru przenikalności elektrycznych. Opracowano metodę korekcji stałych elastycznych i piezoelektrycznych wykorzystującą nieliniowy algorytm najmniejszych kwadratów i zmierzone parametry AFP. Przeprowadzono korekcję stałych elastycznych i piezoelektrycznych kryształu  $\text{NdCa}_4\text{O}(\text{BO}_3)_3$ . Wykazano, że dla stałych skorygowanych różnice między zmierzonymi, a obliczonymi parametrami AFP są bardzo małe.

**Słowa kluczowe:** stałe elastyczne, stałe piezoelektryczne, stałe dielektryczne, akustyczna fala powierzchniowa

## 1. INTRODUCTION

A neodymium calcium oxyborate crystal  $[\text{NdCa}_4\text{O}(\text{BO}_3)_3]$ , abbreviation: NdCOB] shows no phase transition and maintains piezoelectricity up to the melting point of about  $1470^\circ\text{C}$ . It belongs to a monoclinic class, point group  $m$  and is described by 13 elastic, 10 piezoelectric and 4 dielectric constants [1]. These 27 material constants were previously measured by T. Karaki [2] and by F. Yu [3] using the impedance spectroscopy method. A NdCOB crystal is attractive for surface acoustic wave (SAW) components and high temperature sensor applications because some orientations are thermally compensated and show a relatively high electromechanical coupling coefficient, while other orientations are thermally sensitive [4]. In a SAW component design procedure it is important to precisely simulate crystal's SAW properties. Applying constants from [2] or [3] in SAW simulations leads to results that are significantly different, compared to the measured ones. The differences are caused by material constants errors generated during measurements of a large number of differently oriented specimens, relative to the crystal axes. Therefore, the correction of these constants is necessary. The material constants correction based on SAW velocity measurements for such a simple piezoelectric crystal like lithium niobate (trigonal class, point group  $3m$ ) was first proposed in [5]. In this method, SAW velocities for free and metalized crystal surfaces were determined by an optical method. In this work, SAW velocities and electromechanical coupling coefficients were measured using delay lines. Additionally, dielectric constants were evaluated from the measured effective permittivities.

## 2. PRELIMINARY CALCULATIONS

In a monoclinic  $m$  class, a rectangular  $(X, Y, Z)$  coordinate system relative to a crystallographic  $(a, b, c)$  system is chosen such that  $Y \parallel b, Z \parallel c, X$  axis is perpendicular to  $Y$  and  $Z$  axes and forms a right-handed system (Fig. 1a). A SAW-related, right-handed  $(x_1, x_2, x_3)$  system is chosen such that the wave propagates along  $x_1$  axis and decays along  $x_3$  axis (Fig. 1b). The relation (substrate orientation) between  $(X, Y, Z)$  and  $(x_1, x_2, x_3)$  systems is specified by Euler angles  $(\psi, \mu, \theta)$  (Fig. 2).

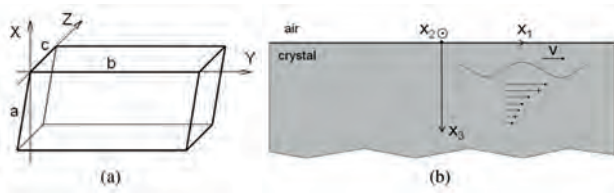


**Fig. 1.** Coordinate system related to crystal axes (a) and to the SAW propagation direction (b).

**Rys. 1.** Układ odniesienia związany z osiami kryształu (a) i z kierunkiem propagacji AFP (b).

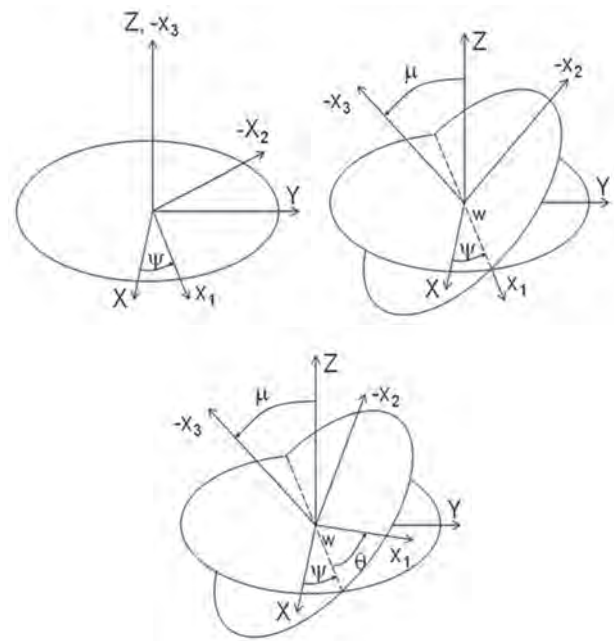


**Fig. 2.** Euler angles definition.

**Rys. 2.** Definicja kątów Eulera.

In [2 - 3] material constants are given in a form of elastic  $s_{ij}^E$ , piezoelectric  $d_{kl}$  and dielectric  $\epsilon_{mn}^T$  (where  $i, j, l = 1, 2, 6; k, m, n = 1, 2, 3$ ; superscripts E and T, which indicate a constant electric field and strain, respectively, will be skipped in the following consideration). When calculating SAW parameters

using an algorithm [6],  $s_{ij}^E, d_{kl}, \epsilon_{mn}^T$  must be transformed into  $c_{ij}^E, e_{kl}, \epsilon_{mn}^S$  constants [7]:

$$[c_{ij}^E] = [s_{ij}^E]^{-1} \quad (1)$$

$$[e_{kl}] = [d_{kl}] \cdot [c_{ij}^E] \quad (2)$$

$$[\epsilon_{mn}^S] = [\epsilon_{mn}^T] - [d_{kl}] \cdot [c_{ij}^E] \cdot [d_{lk}] \quad (3)$$

where  $[s_{ij}^E]^{-1}$  and S indicate an inverse matrix and constant deformation, respectively.

The NdCOB density  $\rho$ , initial  $\epsilon_{mn}^o, s_{ij}^o$  and  $d_{kl}^o$  constants [2 - 3] used in preliminary calculations are shown in Fig. 3.

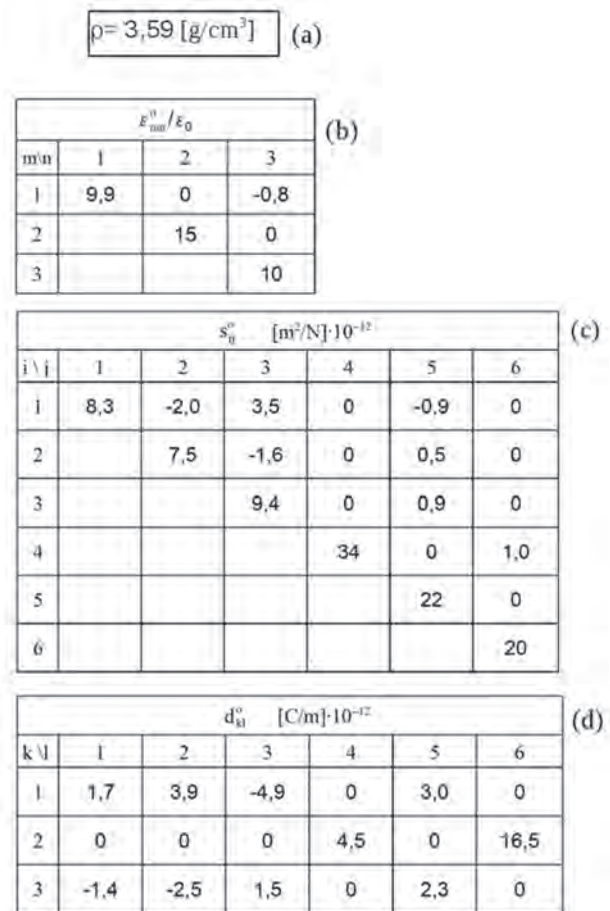


**Fig. 3.** Density (a) and initial dielectric (b), elastic (c) and piezoelectric (d) constants.

**Rys. 3.** Gęstość (a) i początkowe wartości stałych: dielektrycznych (b), elastycznych (c) i piezoelektrycznych (d).

The sensitivity of particular  $s_{ij}$  or  $d_{kl}$  constants in SAW calculation depends on orientation. Computer simulations were carried out to find orientations characterized by the velocity  $v$  and the electromechanical coupling coefficient  $K^2$  sensitive to material constants changes. Calculated  $\Delta v$  and  $\Delta K^2$  changes induced by  $\Delta s_{ij} = \pm 0,01 s_{ij}$  and  $\Delta d_{kl} = \pm 0,01 d_{kl}$  changes, respectively, are shown in Figs. 4 - 5.

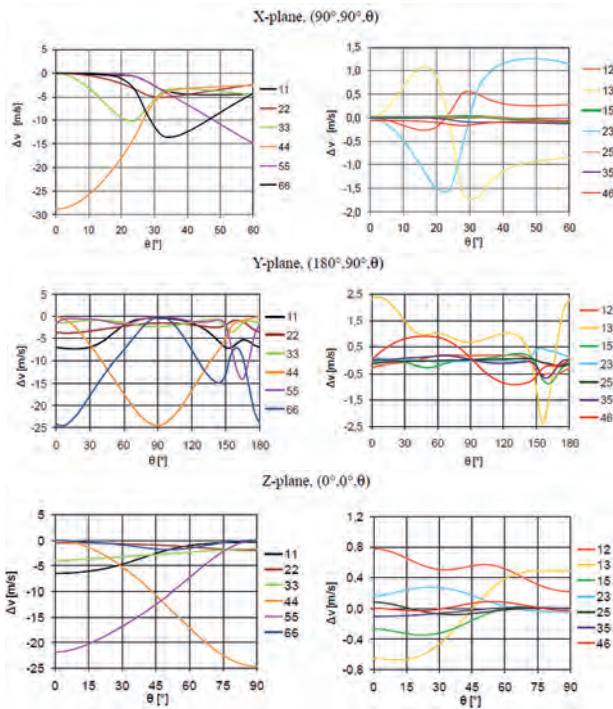


**Fig. 4.** Velocity changes induced by  $\Delta s_{ij} = \pm 0,01s_{ij}$  changes versus the angle  $\theta$  for X-, Y- and Z-planes.

**Rys. 4.** Zmiany prędkości wywołane przez zmiany  $\Delta s_{ij} = \pm 0,01s_{ij}$  w funkcji kąta  $\theta$  w płaszczyznach X, Y i Z.

Velocities for all planes are most sensitive to  $s_{44}$  and  $s_{55}$  changes. For X-plane,  $s_{11}$ ,  $s_{22}$ ,  $s_{33}$ ,  $s_{66}$  induce changes in velocity of about 15 m/s, while  $s_{12}$ ,  $s_{13}$  and  $s_{23}$ , of about 1,5 m/s. For Z-plane,  $s_{11}$  and  $s_{33}$

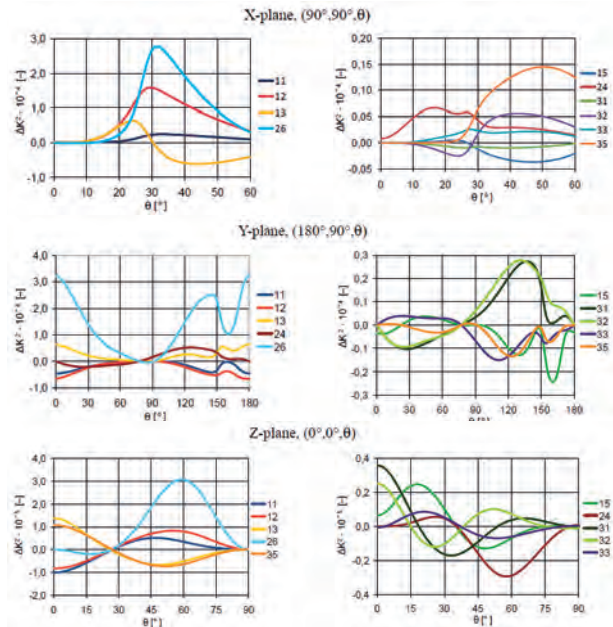


**Fig. 5.** Electromechanical coupling coefficient changes induced by  $\Delta d_{kl} = \pm 0,01d_{kl}$  changes versus the angle  $\theta$  for X-, Y- and Z-planes.

**Rys. 5.** Zmiany współczynnika sprzężenia elektromechanicznego wywołane przez zmiany  $\Delta d_{kl} = \pm 0,01d_{kl}$  w funkcji kąta  $\theta$  w płaszczyznach X, Y i Z.

show medium sensitivity. For Y-plane,  $s_{11}$ ,  $s_{22}$ ,  $s_{66}$  show high sensitivity, while  $s_{13}$  shows low sensitivity. Elastic constants  $s_{15}$ ,  $s_{25}$ ,  $s_{35}$ ,  $s_{46}$  induce very low  $\Delta v$  (below 1m/s), which indicates that they are the constants with the largest uncertainty. Electromechanical coupling coefficient changes induced by  $\Delta d_{kl}$  changes (Fig. 5) are substantial in the case of both X- and Y- planes. For Z-plane,  $\Delta K^2$  is low.

### 3. MEASUREMENT METHOD AND RESULTS

A SAW delay line consisted of two double-electrode inter digital transducers (IDT) and a screen (Fig. 6a) was designed [4] to measure both substrate effective permittivity and SAW properties. The following data were used for the SAW delay line: the period of an electrodes  $p = 8 \mu\text{m}$ , the width of an electrode  $a = \frac{1}{2} p$ , the aperture  $W = 1,6 \text{ mm}$ , the number of electrodes in each IDT and on the screen  $N_t = 254$  and  $N_s = 15$ , respectively. An about  $0,1 \mu\text{m}$  thick aluminum layer was used for metallization.

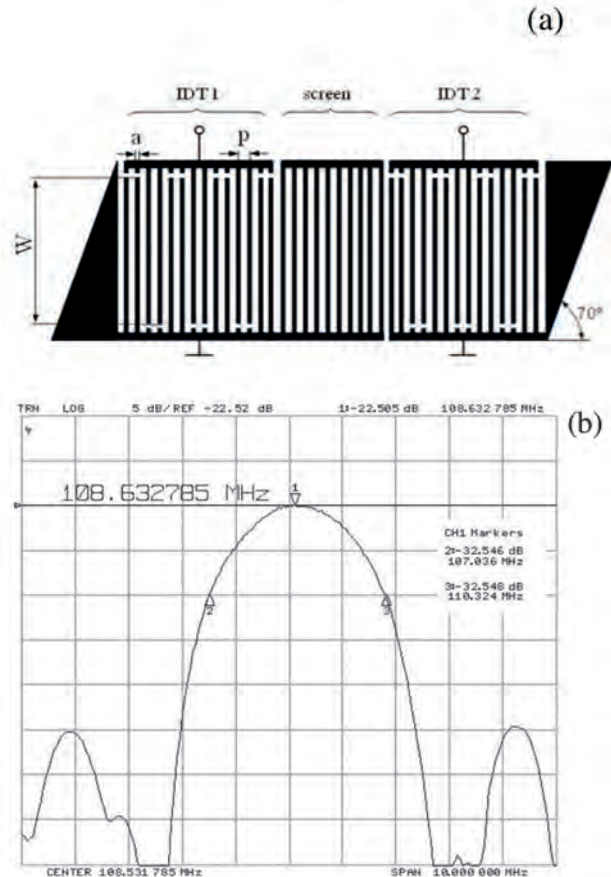


**Fig. 6.** Structure of a delay line (a) and the measured amplitude response of the YX10° NdCOB crystal substrate (b).

**Rys. 6.** Struktura linii opóźniającej (a) i zmierzona charakterystyka amplitudowa podłoża YX10° NdCOB (b).

Amplitude responses were measured using the 50  $\Omega$  system (an Agilent Technologies network analyzer type 8753ET), and an exemplary amplitude response for YX10° orientation is shown in Fig. 6b.

Capacitances of the delay line, needed for the determination of the effective permittivity  $\epsilon_e$ , were measured using a Q-meter (Marconi Instruments). The effective permittivity  $\epsilon_e$  was evaluated from [8]:

$$C_p = 0.707 \cdot W(\epsilon_0 + \epsilon_e)N \quad (3)$$

where  $C_p$  is the transducer capacitance (measured at a frequency of about 5 MHz),  $\epsilon_0$  is the dielectric permittivity of vacuum,  $N = 1/4 N_1$ . Obtained  $\epsilon_e$  for different orientations are shown in Tab. 1. The SAW velocity  $v_m$  under the free surfaced as well as the electromechanical coupling coefficient  $K_m^2$  were determined by comparing the measured and calculated amplitude responses [8]. For each particular orientation, three plates were measured and a mean was calculated as a final result. Obtained values are presented in Tabl. 1. In orientation notation, the first axis is perpendicular to the crystal's plane, the angle is taken between the second axis and the SAW propagation direction. For example, XY20° indicates a plane perpendicular to the X axis and the SAW propagation direction at an angle 20° relative to the Y axis.

**Table 1.** Measured SAW parameters.

**Tabela 1.** Zmierzone parametry AFP.

| n  | Orientation | Euler angles |       |          | $\epsilon_e/\epsilon_0$<br>[-] | $v_m$<br>[m/s] | $K_m^2$<br>[%] |
|----|-------------|--------------|-------|----------|--------------------------------|----------------|----------------|
|    |             | $\psi$       | $\mu$ | $\theta$ |                                |                |                |
| 1  | XY20°       | 90°          | 90°   | 20°      | 10,3                           | 3162           | 0,35           |
| 2  | XY30°       | 90°          | 90°   | 30°      | 10,5                           | 3334           | 1,1            |
| 3  | YX          | 180°         | 90°   | 0°       | 11,9                           | 3510           | 0,7            |
| 4  | YX5°        | 180°         | 90°   | 5°       | 11,7                           | 3497           | 0,56           |
| 5  | YX10°       | 180°         | 90°   | 10°      | 11,5                           | 3483           | 0,5            |
| 6  | YX15°       | 180°         | 90°   | 15°      | 11,4                           | 3432           | 0,45           |
| 7  | YX20°       | 180°         | 90°   | 20°      | 11,2                           | 3377           | 0,44           |
| 8  | YX25°       | 180°         | 90°   | 25°      | 11,1                           | 3345           | 0,4            |
| 9  | YX30°       | 180°         | 90°   | 30°      | 11,1                           | 3280           | 0,36           |
| 10 | YX40°       | 180°         | 90°   | 40°      | 10,7                           | 3180           | 0,3            |
| 11 | YZ          | 180°         | 90°   | 90°      | 12,0                           | 2786           | 0,08           |
| 12 | ZX          | 0°           | 0°    | 0°       | 10,6                           | 3239           | 0,27           |
| 13 | ZY          | 0°           | 0°    | 90°      | 11,8                           | 2780           | 0,08           |

The effective permittivity of the substrate is given by [9]:

$$\epsilon_e = \sqrt{\epsilon'_{11} \cdot \epsilon'_{33} - (\epsilon'_{13})^2} \quad (4)$$

where:  $\epsilon'_{mn}$  is a dielectric permittivity matrix transformed to  $(x_1, x_2, x_3)$  a coordinate system [6]:

$$\epsilon'_{mn} = \sum_{l,s=1}^3 TM_{ml} \cdot TM_{ns} \cdot \epsilon_{ls} \quad (5)$$

where:  $m, n, r, s = 1, 2, 3$ ; TM is a transformation matrix of Euler angles:

$$TM = \begin{pmatrix} \cos\psi \cdot \cos\theta - \sin\psi \cdot \cos\mu \cdot \sin\theta & \sin\psi \cdot \cos\theta + \cos\psi \cdot \cos\mu \cdot \sin\theta & \sin\mu \cdot \sin\theta \\ -\cos\psi \cdot \sin\theta - \sin\psi \cdot \cos\mu \cdot \cos\theta & -\sin\psi \cdot \sin\theta + \cos\psi \cdot \cos\mu \cdot \cos\theta & \sin\mu \cdot \cos\theta \\ \sin\psi \cdot \sin\mu & -\cos\psi \cdot \sin\mu & \cos\mu \end{pmatrix} \quad (6)$$

Dielectric constants  $\epsilon_{mn}$  were obtained by solving a set of equations (4) for different orientations. Obtained dielectric constants are shown in Tab. 2.

**Table 2.** Dielectric constants.

**Tabela 2.** Stałe dielektryczne.

| $\epsilon_{mn}$ | [3]  | [4]  | Measured | Accuracy [%] |
|-----------------|------|------|----------|--------------|
| $\epsilon_{11}$ | 9,9  | 9,9  | 9,9      | ±3           |
| $\epsilon_{13}$ | -0,8 | -1,6 | -1,9     | ±15          |
| $\epsilon_{22}$ | 15   | 15,5 | 15,2     | ±3           |
| $\epsilon_{33}$ | 10   | 10,2 | 9,5      | ±3           |

## 4. CORRECTION PROCEDURE AND RESULTS

It is assumed that the crystal density  $\rho$ , the initial values of elastic  $s_{ij}^0$ , piezoelectric  $d_{ki}^0$  and dielectric  $\epsilon_{mn}^0$  constants are known (Fig. 7). Orientations characterized by the SAW velocity, sensitive to  $s_{ij}^0$  and  $d_{ki}^0$  changes, should be found on the basis of assumed constants. Next, for such oriented crystal substrates, the effective permittivities, the SAW velocities and the electromechanical coupling coefficients ought to be measured. After having performed the measurements, one is advised to fit the calculated SAW velocities to the measured ones using a least squares algorithm. A sum of squares of velocities differences (VSQ) should be taken as the target function:

$$VSQ(s_{ij}) = \sum_n (v_m[n] - v_c[n])^2 \quad (7)$$

where:  $v_c$  and  $v_m$  are the calculated and measured SAW velocities respectively and  $n$  is the orientation number. VSQ must be minimized by elastic constants modification, while piezoelectric constants stay

unchanged at this stage. In the next step, the calculated and measured electromechanical coupling coefficients should be fitted by piezoelectric constants modification. This time, elastic constants, obtained at the previous step, remain unchanged. A sum of squares of electromechanical coupling coefficients (KSQ) ought to be taken as the target function:

$$KSQ(d_{kl}) = \sum_i (K_m^2[n] - K_c^2[n])^2 \quad (8)$$

where:  $K_c^2$  and  $K_m^2$  are the calculated and measured SAW electromechanical coupling coefficients respectively, where:

$$K^2 = 2 \cdot (v_f - v_s) / v_f \quad (9)$$

where:  $v_f$  and  $v_s$  are SAW velocities under free and electrically shorted surface conditions respectively. The minimization procedures ought to be repeated until both VSQ and KSQ reach minimal values.

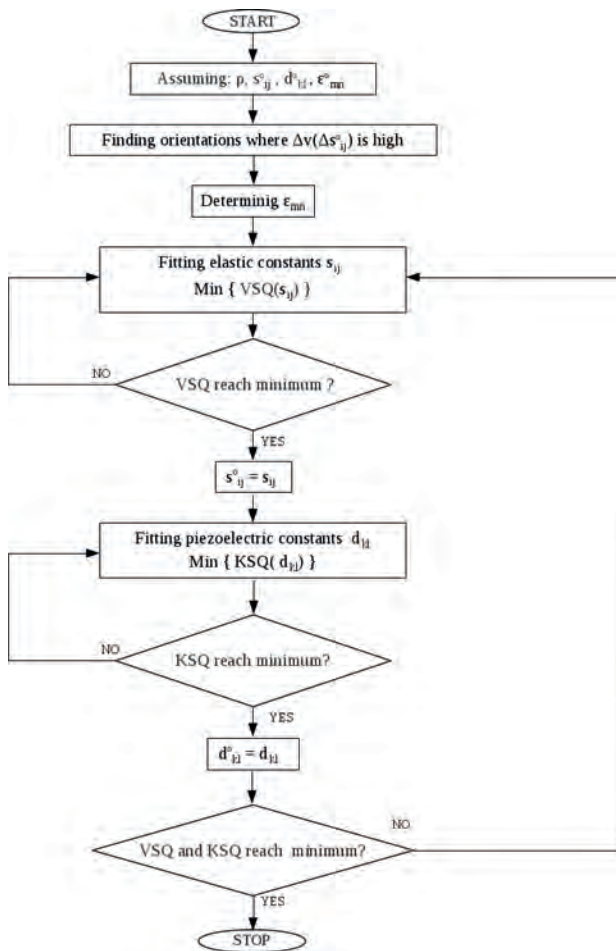


Fig. 7. Correction procedure.

Rys. 7. Procedura korekcji.

An algorithm, invented by R. Hooke and T. Jeeve's [10], was used in the development of the computer

program for both VSQ and KSQ minimization. Corrected elastic and piezoelectric constants are shown in Tab. 3 and Tab. 4 respectively. The differences between the measured and calculated SAW parameters for initial and corrected material constants are presented in Tab. 5.

Table 3. Initial and corrected elastic constants.

Tabela 3. Startowe i skorygowane stałe elastyczne.

| $S_{ij}$ | Initial                                 | Corrected | Accuracy | $C_{ij}^E$<br>$C_{ij}^E$ | Initial                                | Corrected |
|----------|---|-----------|----------|--------------------------|--|-----------|
|          | [m <sup>2</sup> /N] · 10 <sup>-12</sup> |           |          |                          | [N/m <sup>2</sup> ] · 10 <sup>10</sup> |           |
|          |   |           | [%]      |                          |  |           |
| $s_{11}$ | 8,3                                     | 9,310     | ±2       | $c_{11}$                 | 16,5                                   | 12,6      |
| $s_{12}$ | -2                                      | -0,042    | ±15      | $c_{12}$                 | 5,90                                   | 2,18      |
| $s_{13}$ | -3,5                                    | -3,100    | ±9       | $c_{13}$                 | 7,12                                   | 5,40      |
| $s_{15}$ | -0,9                                    | -0,88     | ±20      | $c_{15}$                 | 0,249                                  | 0,233     |
| $s_{22}$ | 7,5                                     | 7,786     | ±3       | $c_{22}$                 | 16,0                                   | 15,4      |
| $s_{23}$ | -1,6                                    | -3,066    | ±15      | $c_{23}$                 | 4,95                                   | 6,48      |
| $s_{25}$ | 0,5                                     | 0,5       | ±27      | $c_{25}$                 | -0,324                                 | -0,514    |
| $s_{33}$ | 9,4                                     | 8,413     | ±3       | $c_{33}$                 | 14,2                                   | 16,3      |
| $s_{35}$ | 0,9                                     | 0,88      | ±31      | $c_{35}$                 | -0,4                                   | -0,574    |
| $s_{44}$ | 34                                      | 33,874    | ±4       | $c_{44}$                 | 2,94                                   | 2,96      |
| $s_{46}$ | 1                                       | 1         | ±24      | $c_{46}$                 | -0,147                                 | -0,16     |
| $s_{55}$ | 22                                      | 22,368    | ±5       | $c_{55}$                 | 4,58                                   | 4,51      |
| $s_{66}$ | 20                                      | 18,889    | ±3       | $c_{66}$                 | 5,00                                   | 5,30      |

Table 4. Initial and corrected piezoelectric constants.

Tabela 4. Startowe i skorygowane stałe piezoelektryczne.

| $d_{kl}$ | Initial                   | Corrected | Accuracy | $e_{kl}$ | Initial | corrected |
|----------|---------------------------|-----------|----------|----------|---------|-----------|
|          | [C/N] · 10 <sup>-12</sup> |           |          |          | [N/C]   |           |
|          |                           |           | [%]      |          |         |           |
| $d_{11}$ | 1,7                       | 1,7       | ±18      | $e_{11}$ | 0,169   | -0,033    |
| $d_{12}$ | 3,9                       | 2,84      | ±8       | $e_{12}$ | 0,472   | 0,076     |
| $d_{13}$ | -4,9                      | -5,87     | ±6       | $e_{13}$ | -0,392  | -0,702    |
| $d_{15}$ | 3,0                       | 3,53      | ±16      | $e_{15}$ | 0,149   | 0,182     |
| $d_{24}$ | 4,5                       | 2,95      | ±12      | $e_{24}$ | 0,108   | 0,059     |
| $d_{26}$ | 16,5                      | 17,78     | ±14      | $e_{26}$ | 0,820   | 0,938     |
| $d_{31}$ | -1,4                      | 0,43      | ±22      | $e_{31}$ | -0,266  | 0,270     |
| $d_{32}$ | -2,5                      | 3,54      | ±26      | $e_{32}$ | -0,416  | 0,690     |
| $d_{33}$ | 1,5                       | 2,39      | ±8       | $e_{33}$ | -0,020  | 0,618     |
| $d_{35}$ | 2,3                       | 4,13      | ±24      | $e_{35}$ | 0,104   | 0,156     |

**Table 5.** Differences between measured and calculated SAW parameters for initial and corrected material constants.

**Tabela 5.** Różnice między zmierzonymi a obliczonymi parametrami AFP dla startowych i skorygowanych stałych materiałowych.

| Orientation | $v_m - v_c$  |  | $K_m^2 - K_c^2$                                    |  |
|-------------|--|--|--|--|
|             | [m/s]  |  | [%] · 10 <sup>2</sup>                              |  |
|             | $s_{ij}^o, d_{kl}^o, \epsilon_{mn}^o$<br>(initial) | $s_{ij}, d_{kl}, \epsilon_{mn}$<br>(corrected) | $s_{ij}^o, d_{kl}^o, \epsilon_{mn}^o$<br>(initial) | $s_{ij}, d_{kl}, \epsilon_{mn}$<br>(corrected) |
| XY20°       | -22,4  | 0,3  | -8,8   | -7,7   |
| XY30°       | -12,2  | -1,6   | 13,4   | 9,9  |
| YX          | 27,4   | -1,4   | -0,8   | 9,8  |
| YX5°        | 11,7   | -3,2   | -9,3   | -3   |
| YX10°       | 7,6  | 6,1  | -6,8   | -2,2   |
| YX15°       | -22,4  | -4,6   | 2,3  | 0,3  |
| YX20°       | -36,7  | -4,5   | 6,1  | 6,4  |
| YX25°       | -39,8  | 4,3  | 3,7  | 1,6  |
| YX30°       | -59,2  | -6,6   | 14,0   | 10,3   |
| YX40°       | -57,5  | 2,2  | 18,5   | 10,8   |
| YZ          | 2,9  | 0,2  | 3,7  | 6,2  |
| ZX          | -26,1  | -3,4   | 25,1   | 6,9  |
| ZY          | -8,5   | -4,3   | -8,0   | -8,2   |

## 5. CONCLUSIONS

Elastic and piezoelectric constants of a NdCOB crystal were corrected by measuring SAW parameters in a chosen orientation set. A nonlinear least squares algorithm was used in the correction procedure. It was shown that for corrected constants the differences between the measured and calculated SAW parameters are slight .

## Acknowledgement

*I would like to thank T. Łukasiewicz, A. Pajczkowska, K. Kłos and M. Gała for crystal growth and substrates fabrication.*

*This work was supported by the National Science Centre under grant No. :N N507 590038.*

## REFERENCES

- [1] Nakao H., Nishida M., Shikida T., Shimizu H., Takeda H., Shiosaki T.: Growth and SAW properties of rare-earth calcium oxoborate crystals, *J. Alloys Compod.*, 408-412, (2006) 582-585
- [2] Karaki T., Adachi M., Kuniyoshi Y.: Evaluation of material constants in NdCa<sub>4</sub>O(BO<sub>3</sub>)<sub>3</sub> piezoelectric single crystal, *J. Electroceram.*, 21, (2008) 823-826
- [3] Yu F., Zhang S., Zhao X., Yuan D., Wang C.-M., Shrout T. R.: Characterization of neodymium calcium oxyborate piezoelectric crystal with monoclinic phase, *Cryst. Growth Des.*, 10, (2010) 1871-1877
- [4] Brzozowski E., Soluch W.: SAW and pseudo SAW properties of NdCa<sub>4</sub>O(BO<sub>3</sub>)<sub>3</sub> crystal, *Electron. Lett.*, 44, (2008) 64-65
- [5] Kovacs G., Trating G., Langer E.: Accurate determination of material constants of piezoelectric crystals from SAW velocity measurements, Proceedings of the IEEE Ultrasonics Symposium, Chicago, IL, USA, October 1988, 269-272
- [6] Campbell J., Jones W. R.: A method for estimating optimal crystal cuts and propagation directions for excitation of piezoelectric surface waves, *IEEE Trans. Sonics Ultrason.*, SU-15, (1968) 209-217
- [7] Auld B.A.: Acoustic fields and waves in solids, John Wiley & Sons, New York, NY, USA, vol. 1, 1973
- [8] Soluch W.: Design of SAW delay lines for sensors, *Sens. Actuators. A*, 67, (1998) 60-64
- [9] Engan H.: Surface acoustic wave multielectrode transducers, *IEEE Trans. Sonics Ultrason.*, 22, (1975) 395-401
- [10] Hook R., Jeeves T.: Direct search solution of numerical and statistical problems, *J. Assoc. Comp. Mach.*, 8, (1961) 221-229